JES Focus Issue on Mechano-Electro-Chemical Coupling in Energy Related Materials and Devices

Mechanical Properties of a Battery Separator under Compression and Tension

John Cannarella,[a,*] Xinyi Liu,[a] Collen Z. Leng,[a] Patrick D. Sinko,[a] Gennady Y. Gor,[b] and Craig B. Arnold[a,,z]**

[a]*Department of Mechanical and Aerospace Engineering, Princeton University, Princeton, New Jersey 08544, USA*
[b]*Department of Civil and Environmental Engineering, Princeton University, Princeton, New Jersey 08544, USA*

Knowledge of the compressive mechanical properties of battery separator membranes is important for understanding their long term performance in battery cells where they are placed under compression. This paper presents a straightforward procedure for measuring the compressive mechanical properties of battery separator membranes using a universal compression testing machine. The compressive mechanical properties of a microporous polypropylene separator are characterized over a range of strain rates and in different fluid environments. These measurements are then compared to measurements of the rate and fluid-dependent mechanical properties of the separator under tension. High strain rate dependence due to viscoelasticity is observed in both tension and compression. An additional rate dependence due to poroelastic effects is observed in compression at high strain rates. A reduction in mechanical properties is observed in DMC solvent environments for both tension and compression, but is found to be less pronounced in compression. The difference in mechanical properties between compression and tension highlight the anisotropic nature of battery separators and the importance of measuring compressive properties in addition to tensile properties.
 [DOI: 10.1149/2.0191411jes] All rights reserved.

Manuscript submitted June 23, 2014; revised manuscript received September 2, 2014. Published September 26, 2014. This was Paper 323 presented at the Orlando, Florida, Meeting of the Society, May 11–15, 2014. *This paper is part of the JES Focus Issue on Mechano-Electro-Chemical Coupling in Energy Related Materials and Devices.*

The battery separator is a porous polymer membrane used to create a physical barrier between electrodes in a battery cell. The separator must be mechanically robust to ensure safe operation over the cell's service life: mechanical failure leading to electrode contact can result in catastrophic failure of the cell.[1-3] Such failure often follows from puncture or thermal shrinkage of the membrane.[4-6] Non-catastrophic battery failure through the form of accelerated degradation can also result from separator deformation.[7-9] The importance of the mechanical properties of the separator with respect to battery safety and durability has consequently motivated much research on the mechanical properties of battery separators.

Previous works on the mechanical properties of separator have mainly investigated the mechanical properties under tension.[10-14] While knowledge of the tensile properties of the separator are important from a manufacturing standpoint, where the separator is placed under tension during cell assembly, the tensile properties are less relevant for general battery operation. This is because the separator is placed under compression during typical battery operating conditions, where it is compressed in the direction normal to the plane of the large separator face by the anode and cathode. This compressive stress is cyclic owing to reversible electrode strains and gradually increases during operation as a result of irreversible volumetric increases occurring on the electrodes.[9,15] These stack stresses during operation have been observed to be on the order of 1MPa in previous work,[9,15,16] although the presence of geometric non-uniformities (e.g. particles and curved faces) can result in local stresses that are significantly higher.[17-19]

The mechanical properties of the separator under normal compression are not expected to be identical to the properties under tension because of the separator's complex anisotropic structure. Similarly, the mechanical behavior of the separator is expected to deviate from the properties of its constituent polypropylene material. For example, a separator membrane manufactured through a dry process consists of many interconnected pore walls that are connected by polymer fibrils that result from the stretching.[20] The stress-strain behavior of a separator should therefore be expected to exhibit behavior characteristic of a cellular material under compression, which is qualitatively distinct from the same material under tension.[21] To date, reports in the literature of compressive properties have been limited to studies on the properties of entire pouch cells[22-25] and a study of the local mechanical properties of a separator using nanoindentation techniques.[26]

This work presents a procedure for characterizing the mechanical properties of a separator under compression. The compressive properties of a microporous polypropylene separator are then characterized under different strain rates and solvent environments. The compressive properties are compared to tensile properties and found to be different. Correct knowledge of these properties can improve models in which the compressive mechanical properties of the separator are important.[17-19,27] Knowledge of the compressive properties can also aid identifying separators and separator materials that might exhibit better long-term performance.

Experimental

Commercially available Celgard 3501 separator is used in all of the mechanical tests presented here. This separator is a monolayer microporous polypropylene (semicrystalline, 40% crystallinity[8]) membrane with a nominal thickness of 25 μm. The Celgard 3501 is manufatured using a dry stretch process and contains a surfactant coating for rapid wetting.[28] In our experience, mechanical tests comparing the behavior of pristine Celgard 3501 and Celgard 3501 rinsed in methanol to remove the surfactant coating produce the same results. Consequently, the surfactant coating is assumed to have little effect on the measured mechanical properties and all data presented here are from separators tested as received.

All mechanical testing is performed using an Instron electromechanical universal testing machine (model 5969). Compression tests are conducted using spherically seated compression platens to maintain good alignment and strain is measured using a LVDT (linear variable differential transformer). Compression tests are conducted on a stack containing multiple layers of separator samples to increase the accuracy of strain measurements and decrease the effects of any misalignment of the platens. Separator samples for compression tests are prepared by folding a separator strip into multiple layers and using an arch punch to cut a 3/8″ diameter disk in the folded stack. Folding prior to punching helps ensure that all the layers in the stack are oriented in the same direction, which is important for repeatable

*Electrochemical Society Student Member.
**Electrochemical Society Active Member.
zE-mail: cbarnold@princeton.edu

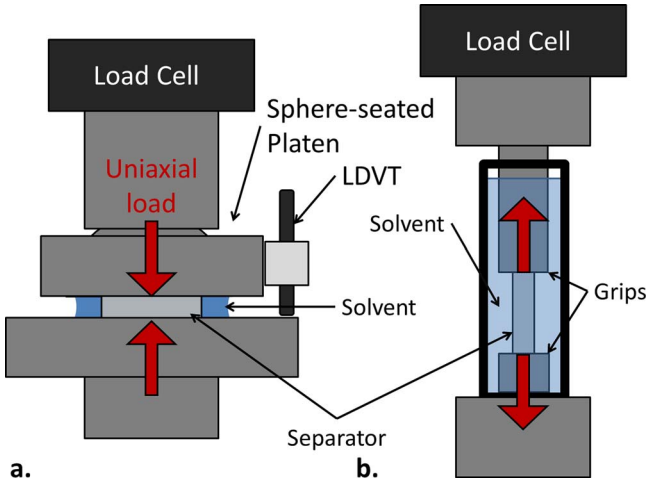

Figure 1. Schematic of test setup used for (a) compressive and (b) tensile stress-strain testing (not to scale).

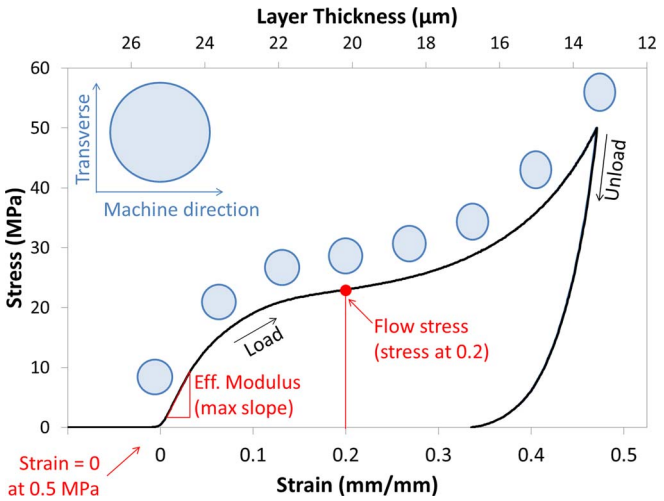

Figure 2. Characteristic stress-strain curve of a separator under compression during loading and unloading. Images showing the progression of the anisotropic separator deformation are overlain. Key properties of the compressive stress-strain curve are marked on the plot.

results due to the anisotropic nature of the separator deformation during compression. The stack of disks is then carefully transferred to the compression testing machine. For determining the effects of sample thickness on measured mechanical properties, all tests are conducted at strain rates of 10^{-2} s^{-1} with variable numbers of separator layers in the stack. A schematic of the compression test setup is shown in Fig. 1a.

For compression tests requiring fluid immersion, fluid is injected between the platens of the compression testing machine and allowed to wet the separator for 20 minutes prior to starting the test. Similar to the work in Ref. 12, we have verified allowing the separator to wet for an additional 24 hours does not produce measurably different mechanical properties. It is verified that there is excess fluid between the platens throughout the duration of the test to ensure that the separator stack remains wet. Mechanical properties are measured using 32 layer stacks at strain rates ranging from 10^{-6} to 1 s^{-1} in dry, water, DMC and 1M $LiPF_6$ in EC/DMC (1:1 by weight) fluid environments. Immersion in DMC is chosen because of its relevance to lithium-ion battery electrolytes and because of its softening effect on tensile properties reported in recent studies on separator properties.[11,12] Immersion in water is chosen to assess the role of chemical interactions between the electrolyte solvents and the separator because water has similar fluidic properties but different chemical properties. Note that due to the reactivity of $LiPF_6$ electrolytes with air, testing $LiPF_6$ electrolyte solution saturated separators is limited to higher rate compression tests, which require relatively short testing times and small volumes of fluid.

Tensile tests are conducted using an in-house tensile fixture that allows in-situ testing in liquid environments, similar in design to that described in Ref. 11. The separator for tensile testing is prepared by using a razor blade to cut the separator into rectangular strips 1cm in width. A gauge length of 2 cm is used during tensile testing. For tests requiring fluid immersion, fluid is filled into the fixture and allowed to wet the separator. It is verified that the fixture contains excess fluid throughout the duration of the test to ensure that the separator remains wet. Tensile tests are conducted in both the machine and transverse directions of the separator at strain rates ranging from 10^{-6} to 1 s^{-1} in dry and DMC fluid environments. A schematic of the tension test setup is shown in Fig. 1b.

Results and Discussion

Stress-strain behavior under compression.— A typical stress-strain curve for a separator under compression during loading and subsequent unloading is shown in Fig. 2. Stress is calculated using the nominal area of the 3/8" disk sample. The strain here is the engineering strain calculated by normalizing deformation of the separator stack by the thickness of the stack at 0.5 MPa. The deformation is measured relative to the thickness at 0.5 MPa, such that strain is defined as 0 mm/mm at 0.5 MPa. We designate the 0.5 MPa thickness as the zero point of the strain measurement so that the unstrained thickness of the separator corresponds to the thickness that would be measured by micrometers, which often have ratcheting mechanisms that limit compressive stress to 0.5 MPa during measurement. Measurements of the thickness of the total separator stack thickness at 0.5MPa suggest there are no gaps between the individual separator layers and compression platens. A secondary X axis is displayed at the top of Fig. 2, which shows the average layer thickness of each separator layer in the stack during the test. This layer thickness is calculated by dividing the separation distance between the platens by the number of separator layers in the stack, and is provided to give the reader an intuitive sense of how the strain corresponds to separator deformation.

The stress-strain curve begins initially with a heel at low stresses as the platens of the compression testing machine make contact with the sample, which is a commonly observed feature in compression testing.[29] Following the initial heel is a region of relatively high slope (marked "Effective Modulus" in Fig. 2) corresponding to elastic deformation of the separator. This steep region contains an inflection point where the slope reaches a maximum and begins to decrease. This change in concavity is attributed to yielding, as experiments in which separators have been deformed past this point show permanent reductions in thickness after unloading. Eventually all the polymer material begins to flow as its yield stress is exceeded resulting in the observed plateau (marked "Flow stress" in Fig. 2). The stress associated with the plateau is below the yield stress that would be expected for bulk polypropylene owing to the porous structure of the material, which dictates that the stress on the actual polymer material is higher than the stress calculated based on the nominal area of the sample. The plateau is upward sloping because as the polymer material flows due to compression, it flows into the pore spaces of the material. This is indicated by the inset images in Fig. 2, which show the shape of the separator (based on before and after measurements) after being deformed to the level of strain indicated by the position of the inset image. The constant macroscopic sample shape during deformation toward the beginning of the plateau indicates that plastic flow occurs into the pore spaces. The decrease in porosity results in a higher stiffness of the material because more material is now bearing the load, manifesting itself as an upward slope in the plateau region.

The plateau ends as the separator densifies due to the flow of the polymer material into the pore spaces, and the stress-strain curve exhibits a higher upward slope. The range of strain over which the plateau

occurs is thus found to be related to the porosity of the separator, with more porous separators exhibiting larger plateaus (not shown here). In this region the separator now must undergo macroscopic deformation in order to accommodate flow of the constituent material, as seen by the change in shape of the macroscopic sample in the inset images in Fig. 2. The macroscopic deformation is anisotropic, following from the anisotropic nature of the manufacturing process. As can be seen in Fig. 2, the separator contracts in the machine direction and expands in the transverse direction. This can be explained by the anisotropic pore structure, which is aligned such that it can internally accommodate flow in the machine direction but not in the transverse direction. Note that these lateral strains are significantly smaller in magnitude than the axial strain applied to the separator stack.

To characterize the rate dependence of the separator mechanical properties, we focus on the effective modulus and flow stress, which are defined as shown in Fig. 2. These two parameters are chosen because they are characteristic of the major features of the separator stress-strain curve. We define the effective modulus as the maximum slope of the stress-strain curve between the low and high stress plateaus. Note that this is a measure of the stiffness of the separator structure, and is not the same as the Young's modulus of the polypropylene material that comprises the structure. We define the flow stress as the stress at 0.2 mm/mm strain, which is characteristic of the high stress plateau. This definition of flow stress is used in lieu of a yield stress (typically defined as the stress at which the stress-strain curve deviates from linear-elastic behavior) because the separator stress-strain curves generally do not exhibit ideal linear-elastic behavior, which makes determination of a yield point difficult. It is important to note that the flow stress defined here is not the stress at which the onset of plastic deformation occurs, but is defined to be characteristic of the plateau feature in the separator stress-strain curve. This type of flow stress definition is common practice in compressive testing of cellular plastics as designated by ASTM standard D1621.[29]

All compression tests are conducted on stacks containing multiple layers of separator. Multiple layers are used because compression testing of a single 25 μm separator membrane is not feasible in a typical compression testing machine. Compression testing of a single layer would be preferable if possible, as a single layer more closely resembles the boundary conditions in a real battery cell in which a single separator layer is compressed by two rigid electrodes. Using multiple separator layers increases the accuracy of the strain measurements and decreases any effects that might arise from misalignment of the platens. One issue of concern when conducting these compression tests is how the thickness of the stack effects the measured mechanical properties. To determine the influence of stack thickness on the measured compressive properties, stacks consisting of different numbers of separator layers are tested. The variation in flow stress and effective modulus as a function of the number of separator layers in the stack is shown in Fig. 3. All mechanical properties show decreases at low sample thicknesses, which is attributed to possible edge effects and platen misalignment. After 32 layers, the variation in mechanical properties with sample thickness begins to decay. We choose 32 layers as the standard sample thickness because it offers a balance between reduction of edge effects and ease of handling. Above 32 layers, it becomes difficult to prepare samples repeatedly.

Rate dependence of mechanical properties.— The mechanical properties of the polymer separators are rate-dependent, and are consequently measured at strain rates spanning many orders of magnitude in this work. To provide the reader with an intuitive sense of how these strain rates are related to charging rates in a battery cell, we can calculate an equivalent C-rate corresponding to each strain rate. We calculate this rate based on the LCO/C pouch cell described in Ref. 30. Fig. 2b of Ref. 30 shows the cell expands during constant current charging at a rate of approximately 0.8 and 0.6 mm/Ah at low and high states of charge, respectively. We assume that if the cell were constrained, all of the measured expansion would be accommodated by the cell's separator, which has a cumulative thickness of 0.48 mm (17 layers, 2 faces per layer, 0.014 mm separator thickness). Using a "characteristic" expansion of 0.7 mm/mAh and calculating C-rate based on the cell's 240 mAh capacity gives an equivalent strain rate of 10^{-4} s^{-1} for a 1C rate. Thus a strain rate of 10^{-5} s^{-1} corresponds to a C/10 rate, 10^{-3} s^{-1} corresponds to 10C, and so on. Note that this is a rough estimate which does not include deformation of other components in the cell stack, thermal expansion, or the concentration-dependent expansion behavior of the materials, which are also important factors in determining cell expansion.[31] Nevertheless, we believe this "rule of thumb" conversion to be reasonable in providing an order of magnitude estimate for constrained LCO/C systems. For higher expansion materials, the equivalent C-rate would be lower for a given strain rate.

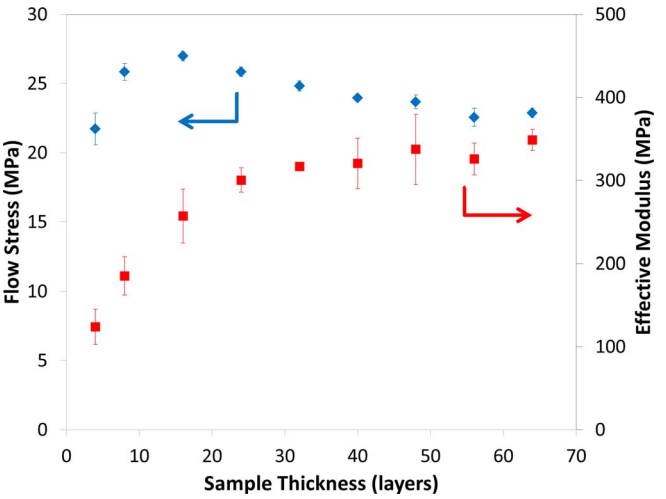

Figure 3. Flow stress and effective modulus as a function of number of separator layers comprising the sample stack for compression testing. Each data point represents an average of 5 samples. Error bars represent +/− one standard deviation.

To illustrate the strain-rate dependent mechanical behavior of fluid-immersed separators, a family of stress-strain curves at different strain-rates for a separator immersed in DMC is shown in Fig. 4. Figure 4 shows a general trend of increased mechanical properties with higher strain rates, with a particularly large rate of increase at strain rates above 10^{-3} s^{-1}. The variation of these curves with strain rate is generally representative of all of the fluid-immersed separators tested in this work. However, plotting stress-strain curves for every sample would yield unwieldy figures, and only the characteristic properties of effective modulus and flow stress are plotted in the subsequent figures. The effective modulus and flow stress as a function of strain rate are shown in Fig. 5 for separators immersed in electrolyte, DMC, and water, as

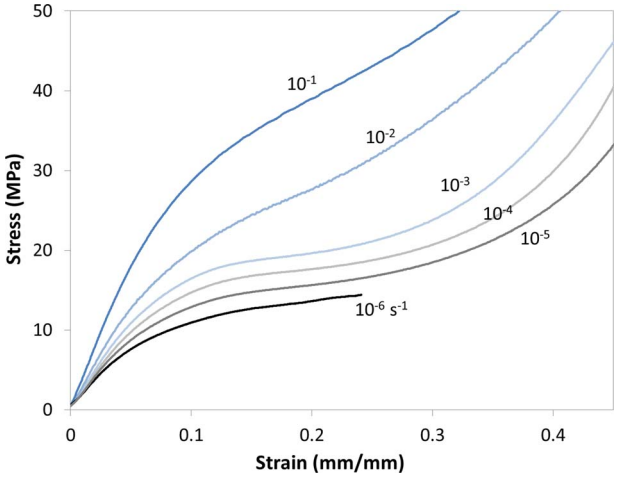

Figure 4. Compressive stress-strain curves of a separator immersed in DMC at different strain rates.

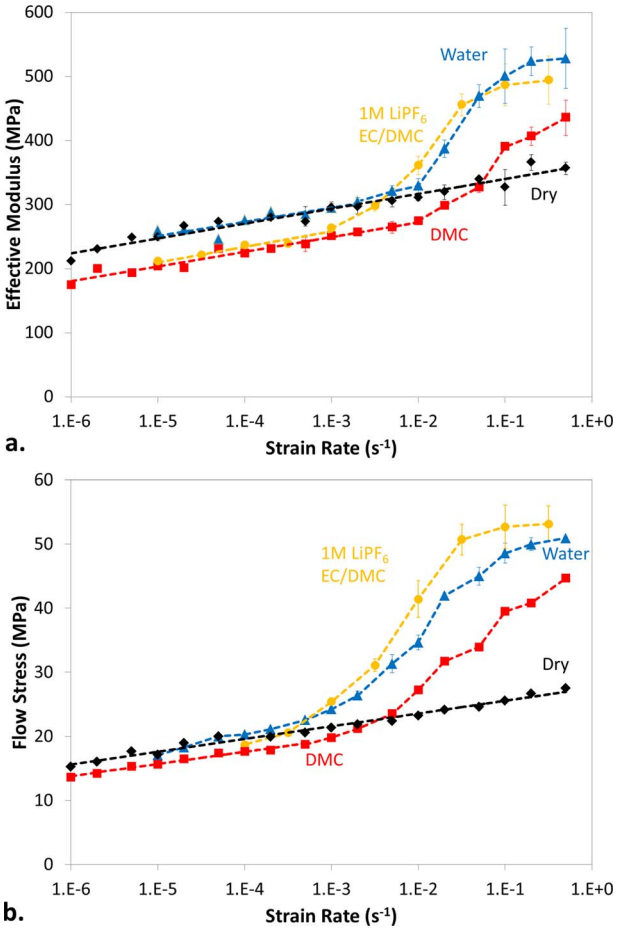

Figure 5. Compressive mechanical properties (a) effective modulus and (b) flow stress for a stack of 32 separators as a function of strain rate. Error bars indicate +/− one standard deviation on a data point representing an average of multiple samples as indicated in Table I.

well as in the dry condition. At low strain rates, the separators show a linear scaling of effective modulus and flow stress with logarithm of strain rate. A similar dependence for the yield stress was reported in[11] for tensile measurements of a polyolefin separator, and is attributed to viscoelastic effects. It is interesting to note that the same scaling between mechanical properties and strain rate is exhibited between the dry separator and all of the fluid-immersed separators. This suggests that the properties of the electrolyte-immersed separator, which are not measured at lower strain rates due to its reactivity, can be determined through extrapolation based on the rate-dependent measurements of the dry or DMC-immersed separators.

While the low strain rate rate-dependence is attributed to viscoelasticity, the observed scaling cannot be explained by the typically-used linear viscoelastic models based on Hookean springs and Newtonian dashpots. The logarithmic scaling can, however, be explained in the context of Eyring's theory, in which a polymer's viscosity is an exponential function of applied stress.[32] The variable viscosity used in Eyring's theory is necessary because the viscous properties of rubber-like and semicrystalline polymers[33,34] deviate from Newtonian behavior, and change as a function of applied stress. This predictable scaling suggests that the measured mechanical properties at higher strain rates can be used to determine the mechanical properties at much lower strain rates. Exploitation of such a relationship can save large amounts of time in mechanical characterization of the separator, as low strain rate tests can take multiple weeks or longer.

Role of fluid in compressive testing.— The fluid-immersed separators show an additional rate-dependent stiffening at high strain rates that is not present in the dry separators. This effect is well-known for porous systems saturated with fluid and can be understood within the theory of porelasticity.[35] Poroelastic behavior is related to the fluid flow in the pores. When the porous body saturated with fluid is compressed slowly, the fluid has enough time to flow out from the pores (drained response). However, at fast compression, when the fluid does not have enough time to escape from the pores, it gets compressed in the pores. In this case the porous body becomes effectively stiffer (undrained response). Because poroelastic stiffening effects are caused by resistance to fluid flow in the pores of the electrolyte, decreasing the permeability of the membrane or increasing the viscosity of the fluid will both result in a higher stiffness at a given strain rate.

The effect of viscosity is apparent in Fig. 5, in which poroelastic stiffening becomes noticeable at progressively lower strain rates for the electrolyte (4.2 mPa · s[36]), water (1 mPa·s), and DMC (0.6 mPa · s), following a trend of higher viscosity. For the case of the electrolyte solution, Fig. 5 shows that poroelastic effects become important at strain rates $\gtrsim 10^{-3}$ s^{-1} (C-rates $\gtrsim$ 10C) for the 1cm diameter separator samples. Poroelastic effects become increasingly important when considering larger format cells where the length scales for fluid drainage are much larger than the samples used here, as well as higher rate operation, more viscous electrolyte solutions, and high rate loading scenarios such as impact. Finite element modeling of these effects are discussed in Ref. 37.

Figure 5 also shows that immersion of the separator in DMC and in the $LiPF_6$ electrolyte solution results in weakening of mechanical properties compared to the dry separator, with electrolyte/DMC-immersed values ranging from 75% to 90% of their dry values. As has been observed in previous work, immersion in DMC results in comparable softening to immersion in 1M $LiPF_6$ in EC/DMC (1:1), with DMC exhibiting a marginally greater softening.[12] These weakening effects are observed at strain rates $\lesssim 10^{-3}$ s^{-1}, where poroelastic stiffening effects due to fluid immersion are unimportant. However, even at high strain rates when the poroelastic effects come into play, the effective modulus of elelectrolyte/DMC-immersed separator is lower than that of the water-immersed. This shows that the softening of the separator has chemical origin and is related to specific interactions between the solvent molecules and the separator. Similar softening effects in polypropylene separators due to DMC immersion have been observed previously in both experimental work[11,12] and in silico.[38]

Comparison of compressive and tensile properties.— We also measure the mechanical properties as a function of strain rate in different solutions in order to allow comparison of the compressive mechanical properties to the tensile mechanical properties of the separator. Figure 6 shows a family of stress-strain curves for DMC-immersed separators in the machine and tensile directions at different strain

Table I. Table listing the number of samples represented by each data point in Fig. 5.

−log(ε̇):	6	5.7	5.3	5	4.7	4.3	4	3.7	3.3	3	2.7	2.3	2	1.7	1.3	1	0.7	0.3	total
DMC	1	1	1	1	1	1	1	1	2	3	5	5	5	6	3	3	3	4	47
Dry	1	1	1	2	1	1	1	1	2	3	5	5	5	6	3	7	4	3	52
Water	1	1	1	1	1	1	1	1	2	2	3	3	3	3	3	3	5	2	37
				5		4.5		4		3.5		3		2.5		2		1.5	1		0.5		
1M LiPF6 (EC:DMC)				1		1		1		1		4		4		4		5	4		5		30

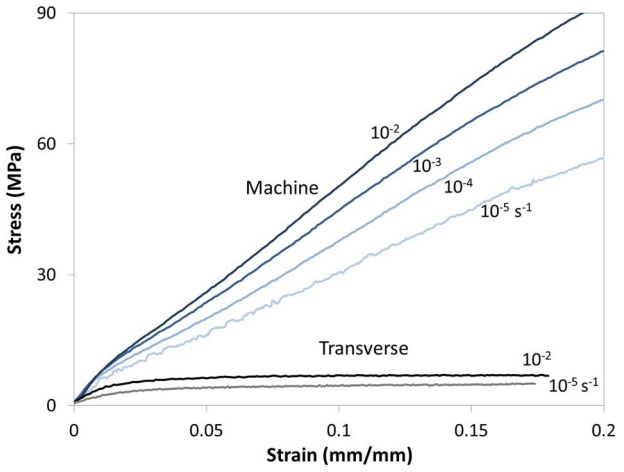

Figure 6. Tensile stress-strain curves at different strain rates of a separator immersed in DMC for both the machine and transverse directions.

rates. These tensile stress-strain curves are qualitatively similar to those presented in previous work investigating the tensile properties of microporous Celgard separators.[11-14] The tensile mechanical behavior of all of the tested separators is summarized in Figs. 7 and 8, which show effective modulus and flow stress at different strain rates for separators tested in the machine and transverse direction, respectively. The effective modulus is again calculated as the maximum slope of the stress strain curve prior to yielding. For the transverse direction, an obvious yield stress is present, and the average stress of the plateau (seen in the transverse direction stress-strain curves in Fig. 8) is used as the flow stress similar to previous studies.[11,12] For the machine direction, the flow stress is defined at 0.2 mm/mm strain as is done for the case of compression presented previously in this work.

The tensile properties plotted in Figs. 7 and 8 are generally consistent with those reported previously in the literature with respect to magnitude and effect of solvent immersion.[12] However, there are some notable differences between the mechanical properties of the separator measured in tension compared with those measured in compression. The first notable difference is the magnitude of the measured effective modulus, which is lower when measured in compression than when measured in tension in both the transverse and machine directions. The effective modulus in compression is more similar in value to the effective modulus in the transverse direction under tension, which

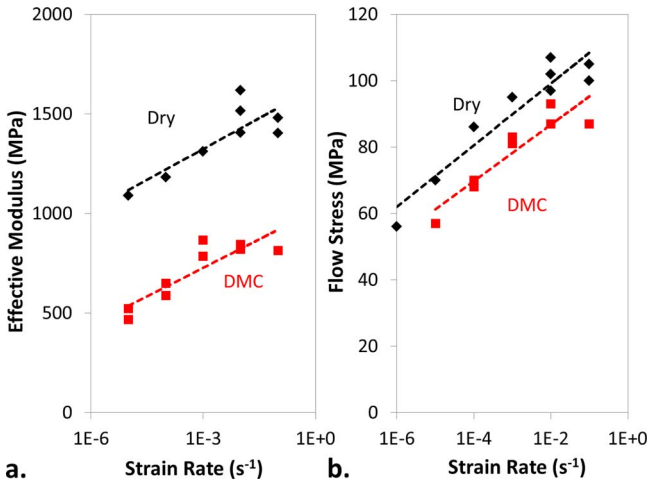

Figure 7. Machine direction tensile mechanical properties (a) effective modulus and (b) flow stress for a separator as a function of strain rate. Each data point represents an individual test.

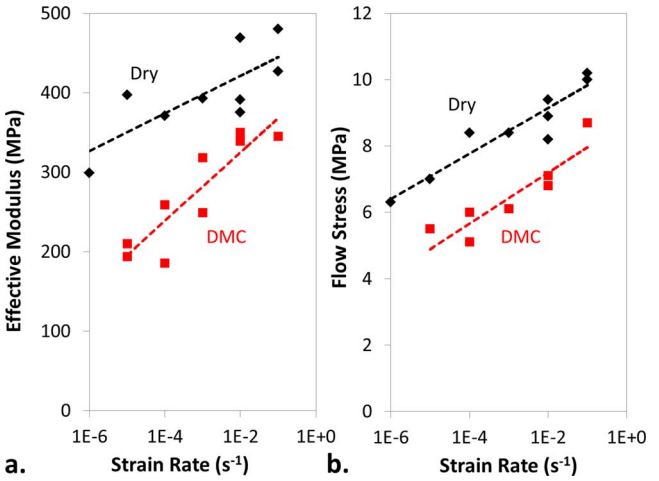

Figure 8. Transverse direction tensile mechanical properties (a) effective modulus and (b) flow stress for a separator under tension in the transverse direction as a function of strain rate. Each data point represents an individual test.

should be expected because both scenarios load the separator in directions that have not been strain-hardened in manufacturing the porous structure. This is in contrast to the effective modulus in the machine direction, which is significantly strengthened through the stretching process during manufacturing.

While the tensile properties plotted in Figs. 7 and 8 show a similar scaling with strain rate as the compressive properties in Fig. 5, there is a notable absence of poroelastic effects in tension over the measured strain rates. This is indicated by the absence of an upward deviation from the linear relationships at high strain rates in Figs. 7 and 8, which would be characteristic of poroelastic stiffening. The absence of poroelastic effects is expected because the characteristic length of fluid flow under tension (on the scale of 25 μm separator thickness) is much smaller than the characteristic length of fluid flow under compression (on the scale of ∼1 cm sample radius). This is many orders of magnitude lower than the characteristic length (macroscopic sample radius) of the separators under compression.

Finally, the effects of swelling are much less pronounced in compression than in tension. In tensile measurements in both the machine direction and transverse direction, both effective modulus and flow stress are between 50% and 60% of their dry values when immersed in DMC. This is in contrast to the the case of compression, where the DMC-immersed mechanical properties are between 75% and 90% of their dry values. The notable differences in mechanical properties between compression and tension highlights the anisotropic nature of the separator mechanical properties and emphasizes the importance of measuring the compressive properties of the separator instead of using tensile properties as a proxy for compression.

Conclusions

Battery separators are a challenge for compression testing owing to their non-ideal properties such as porosity, viscoelasticity, solvent-immersion dependence, and small thickness. This work addresses the challenges in measuring the compressive mechanical properties of battery separators by developing a procedure for characterizing the membranes that can be easily reproduced in other laboratories. The compressive stress-strain behavior, rate dependence, and solvent-immersion dependence of a Celgard polypropylene microporous separator are characterized. The behavior of the separator in compression is found to be different in tension, demonstrating that the tensile properties cannot necessarily be used as a proxy for the compressive properties of the separator. In particular, the softening effects due to polymer-solvent interactions for separators are much more pronounced in tension than in compression. Knowledge of the

compressive properties of various separators can allow for better understanding of the long-term performance of separators in real battery cells where they operate under compressive loads.

Acknowledgments

J.C. acknowledges the Department of Defense (DoD) for support through the National Defense Science and Engineering Graduate Fellowship (NDSEG) Program. We acknowledge support from the Princeton University Siebel Energy Grand Challenge and the Princeton University Carbon Mitigation Initiative. J.C. also acknowledges the Rutgers-Princeton NSF IGERT in Nanotechnology for Clean Energy. We also acknowledge support from the Addy Fund through the Andlinger Center for Energy and the Environment.

References

1. X. Huang, "Separator technologies for lithium-ion batteries," *J. Solid State Electrochem.*, **15**(4), 649 (2010).
2. S. S. Zhang, "A review on the separators of liquid electrolyte Li-ion batteries," *J. Power Sources*, **164**(1), 351 (2007).
3. P. Arora and Z. J. Zhang, "Battery separators," *Chem. Rev.*, **104**(10), 4419 (2004).
4. E. Sahraei, J. Meier, and T. Wierzbicki, "Characterizing and modeling mechanical properties and onset of short circuit for three types of lithium-ion pouch cells," *J. Power Sources*, **247**, 503 (2014).
5. E. Sahraei, J. Campbell, and T. Wierzbicki, "Modeling and short circuit detection of 18650 Li-ion cells under mechanical abuse conditions," *J. Power Sources*, **220**, 360 (2012).
6. W. Cai, H. Wang, H. Maleki, J. Howard, and E. Lara-Curzio, "Experimental simulation of internal short circuit in li-ion and li-ion-polymer cells," *J. Power Sources*, **196**(18), 7779 (2011).
7. C. Peabody and C. B. Arnold, "The role of mechanically induced separator creep in lithium-ion battery capacity fade," *J. Power Sources*, **196**(19), 8147 (2011).
8. J. Cannarella and C. B. Arnold, "Ion transport restriction in mechanically strained separator membranes," *J. Power Sources*, **226**, 149 (2013).
9. J. Cannarella and C. B. Arnold, "Stress evolution and capacity fade in constrained lithium-ion pouch cells," *J. Power Sources*, **245**, 745 (2014).
10. J. Chen, Y. Yan, T. Sun, Y. Qi, and X. Li, "Deformation and fracture behaviors of microporous polymer separators for lithium ion batteries," *RSC Advances*, **4**(29), 14904 (2014).
11. I. Avdeev, M. Martinsen, and A. Francis, "Rate- and Temperature-Dependent Material Behavior of a Multilayer Polymer Battery Separator," *J. Mater. Eng. Perform.*, **23**(1), 315 (2014).
12. A. Sheidaei, X. Xiao, X. Huang, and J. Hitt, "Mechanical behavior of a battery separator in electrolyte solutions," *J. Power Sources*, **196**(20), 8728 (2011).
13. C. T. Love, "Thermomechanical analysis and durability of commercial micro-porous polymer Li-ion battery separators," *J. Power Sources*, **(5)**, 2905 (2011).
14. G. Venugopal, J. Moore, J. Howard, and S. Pendalwar, "Characterization of microporous separators for lithium-ion batteries," *J. Power Sources*, **77**(1), 34 (1999).
15. J. Cannarella and C. B. Arnold, "State of health and charge measurements in lithium-ion batteries using mechanical stress," *J. Power Sources*, **269**, 7 (2014).
16. X. Wang, Y. Sone, G. Segami, H. Naito, C. Yamada, and K. Kibe, "Understanding Volume Change in Lithium-Ion Cells during Charging and Discharging Using In Situ Measurements," *J. Electrochem. Soc.*, **154**(1), A14 (2007).
17. W. Wu, X. Xiao, X. Huang, and S. Yan, "A multiphysics model for the in situ stress analysis of the separator in a lithium-ion battery cell," *Comput. Mater. Sci.*, **83**, 127 (2014).
18. D. Shi, X. Xiao, X. Huang, and H. Kia, "Modeling stresses in the separator of a pouch lithium-ion cell," *J. Power Sources*, **196**(19), 8129 (2011).
19. X. Xiao, W. Wu, and X. Huang, "A multi-scale approach for the stress analysis of polymeric separators in a lithium-ion battery," *J. Power Sources*, **195**(22), 7649 (2010).
20. H. S. Bierenbaum, R. B. Isaacson, M. L. Druin, and S. G. Piovan, "Microporous Polymeric Films," *Ind. Eng. Chem. Prod. Res. Dev.*, **13**(1), 2 (1974).
21. L. J. Gibson and M. F. Ashby, *Cellular solids: structure and properties*, Cambridge University Press, 1999.
22. T. Wierzbicki and E. Sahraei, "Calibration of the Mechanical Properties of the Jellyroll from Crush Tests on Cylindrical Li-ion Cells," *J. Power Sources*, **241**, 467 (2013).
23. T. Wierzbicki and E. Sahraei, "Homogenized mechanical properties for the jellyroll of cylindrical Lithium-ion cells," *J. Power Sources*, **241**, 467 (2013).
24. E. Sahraei, R. Hill, and T. Wierzbicki, "Calibration and finite element simulation of pouch lithium-ion batteries for mechanical integrity," *J. Power Sources*, **201**, 307 (2012).
25. L. Greve and C. Fehrenbach, "Mechanical testing and macro-mechanical finite element simulation of the deformation, fracture, and short circuit initiation of cylindrical Lithium ion battery cells," *J. Power Sources*, **214**, 377 (2012).
26. I. C. Halalay, M. J. Lukitsch, M. P. Balogh, and C. A. Wong, "Nanoindentation testing of separators for lithium-ion batteries," *J. Power Sources*, **238**, 469 (2013).
27. Y. Pan and Z. Zhong, "Modeling the Ion Transport Restriction in Mechanically Strained Separator Membranes," *J. Electrochem. Soc.*, **161**(4), A583 (2014).
28. www.celgard.com.
29. ASTMInternational, Standard test method for compressive properties of rigid cellular plastics, Designation: D1621-10.
30. J. Cannarella, C. Z. Leng, and C. B. Arnold, "On the coupling between stress and voltage in lithium-ion pouch cells," *Proc. of SPIE*, **9115**, 91150K (2014).
31. K.-Y. Oh, J. B. Siegel, L. Secondo, S. U. Kim, N. a. Samad, J. Qin, D. Anderson, K. Garikipati, A. Knobloch, B. I. Epureanu, C. W. Monroe, and A. Stefanopoulou, "Rate Dependence of Swelling in Lithium-ion Cells," *J. Power Sources*, **267**, 197 (2014).
32. H. Eyring, "Viscosity, plasticity, and diffusion as examples of absolute reaction rates," *J. Chem. Phys.*, **4**(4), 283 (1936).
33. A. Tobolsky and H. Eyring, "Mechanical properties of polymeric materials," *J. Chem. Phys.*, **11**(3), 125 (1943).
34. I. M. Ward and J. Sweeney, *Mechanical properties of solid polymers*, John Wiley & Sons, 2012.
35. O. Coussy, *Poromechanics*, John Wiley & Sons, 2004.
36. Y. R. Dougassa, J. Jacquemin, L. El Ouatani, C. Tessier, and M. Anouti, "Viscosity and carbon dioxide solubility for lipf6, litfsi, and lifap in alkyl carbonates: Lithium salt nature and concentration effect," *J. Phys. Chem. B*, **118**(14), 3973 (2014).
37. G. Y. Gor, J. Cannarella, J. H. Prévost, and C. B. Arnold, "A model for the behavior of battery separators in compression at different strain/charge rates," *J. Electrochem. Soc.*, this issue.
38. S. Yan, X. Xiao, X. Huang, X. Li, and Y. Qi, Unveiling the environment-dependent mechanical properties of porous polypropylene separators Submitted.